Symmetry Violation of Quantum Multifractality: Gaussian fluctuations versus Algebraic Localization

A. M. Bilen, B. Georgeot, O. Giraud, G. Lemarié, A. M. Bilen, B. Georgeot, O. Giraud, G. Lemarié, A. M. Bilen, B. Georgeot, O. Giraud, G. Lemarié, A. M. Bilen, B. Georgeot, O. Giraud, G. Lemarié, A. M. Bilen, B. Georgeot, A. M. Bilen, B. Georgeot, D. Giraud, G. Lemarié, A. M. Bilen, B. Georgeot, A. M. Bilen, B. Georgeot, D. Giraud, G. Lemarié, A. M. Bilen, B. Georgeot, D. Giraud, G. Lemarié, A. M. Bilen, B. Georgeot, D. Giraud, G. Lemarié, A. M. Bilen, B. Georgeot, D. Giraud, G. Lemarié, A. M. Bilen, B. Georgeot, D. Giraud, G. Lemarié, A. M. Bilen, B. Georgeot, D. Giraud, G. Lemarié, A. M. Bilen, B. Georgeot, D. Giraud, G. Lemarié, A. M. Bilen, B. Georgeot, D. Giraud, G. G. Lemarié, A. M. Bilen, B. Georgeot, D. Giraud, G. G. Lemarié, A. M. Bilen, B. Georgeot, D. Giraud, G. G. G. Giraud, G. Giraud, G. Giraud, G. G. Giraud, G. G. Giraud, G. G. Giraud, G. Giraud, G. Giraud, G. G. Giraud, G. Giraud, G. Giraud, G. G. Giraud, G. G. Giraud, G. Giraud, G. Giraud, G. G. Giraud, G.

¹Instituto de Investigaciones Físicas de Mar del Plata (IFIMAR), Facultad de Ciencias Exactas y Naturales, Universidad Nacional de Mar del Plata and CONICET, Funes 3350, B7602AYL Mar del Plata, Argentina.

²Laboratoire de Physique Théorique, Université de Toulouse, CNRS, UPS, France

³Université Paris Saclay, CNRS, LPTMS, 91405, Orsay, France

⁴MajuLab, CNRS-UCA-SU-NUS-NTU International Joint Research Unit, Singapore

⁵Centre for Quantum Technologies, National University of Singapore, Singapore

(Dated: May 1, 2022)

Quantum multifractality is a fundamental property of systems such as non-interacting disordered systems at an Anderson transition and many-body systems in Hilbert space. Here we discuss the origin of the presence or absence of a fundamental symmetry related to this property. The anomalous multifractal dimension Δ_q is used to characterize the structure of quantum states in such systems. Although the multifractal symmetry relation $\Delta_q = \Delta_{1-q}$ is universally fulfilled in many known systems, recently some important examples have emerged where it does not hold. We show that the reason for this is the presence of atypically small eigenfunction amplitudes induced by two different mechanisms. The first one was already known and is related to Gaussian fluctuations well described by random matrix theory. The second one, not previously explored, is related to the presence of an algebraically localized envelope. While the effect of Gaussian fluctuations can be removed by coarse graining, the second mechanism is robust to such a procedure. We illustrate the violation of the symmetry due to algebraic localization on two systems of very different nature, a 1D Floquet critical system and a model corresponding to Anderson localization on random graphs.

PACS numbers: 05.45.Df, 05.45.Mt, 71.30.+h, 05.40.-a

The structure of eigenfunctions is a remarkable aspect of quantum systems with critical behavior, as exemplified by Anderson localization in disordered quantum systems [1]. In that setting, consisting of noninteracting particles in a disordered potential, as either disorder or energy is varied, the single-particle wave functions go from being extended to exponentially localized in real space, whereas for a critical value of the parameters they present scale-invariant fluctuations [2], a property called multifractality [3-5]. Recently, it was found that many-body states exhibit multifractal properties in Hilbert space. This is quite generic for ground states [6–11], but is also characteristic of highly excited states in the many-body localization regime [12, 13], a subject [14-17] of strong interest due to its implications in quantum statistical mechanics. Multifractality has also interesting potential applications for quantum computing [18].

Multifractality of quantum states ψ can be defined through the scaling of the inverse participation ratios (IPR)

$$I_q(N) \equiv \sum_{r=1}^{N} \langle |\psi_r|^{2q} \rangle \sim N^{-\Delta_q + 1 - q} \tag{1}$$

with N the size of the system, $q \in \mathbb{R}$ and $\langle \cdot \rangle$ indicating an average over disorder and eigenstates. The so-called anomalous dimensions Δ_q quantify the deviation from an ergodic behavior for which $\Delta_q = 0$ since $\langle |\psi_r|^2 \rangle \sim N^{-1}$ for all r. For an exponentially localized state, $\Delta_q = 1 - q$ for q > 0 and $\Delta_q = -\infty$ for q < 0. Aside from these two extremes, a multifractal state possesses scale-invariant fluctuations characterized by a set of anomalous dimensions Δ_q with a non-trivial dependence on q.

An important property of quantum multifractality is the

symmetry relation

$$\Delta_q = \Delta_{1-q} \,. \tag{2}$$

It was first derived from a more general symmetry for the local density of states for nonlinear σ -models [19]. It can also be seen as a consequence of the conformal invariance of random critical points [20, 21]. An alternative viewpoint connects it with fluctuation relations of the Gallavotti-Cohen type [22]. These theoretical results and their numerical verification in very distinct physical systems (like Anderson transitions in 2D and 3D [23–26], quantum Hall transition [27], random graphs [28, 29], and random matrix models [19, 30, 31]), with the addition of its experimental verification for the Anderson transition in sound waves [32], support the argument in favor of the universality of Eq. (2).

However, for several systems Eq. (2) does not hold. Prominent examples are the non-ergodic extended phase of the Anderson model on the Cayley tree [29, 33]; the localized regime of the Anderson model on random graphs [29, 33, 34], which has recently attracted strong interest due to its relation to many-body localization; and 1D Floquet critical systems known as pseudo-integrable [30, 35, 36].

In this letter we focus on these last two models. We observe that the unifying cause of the violation of Eq. (2) is the presence of atypically small eigenfunction amplitudes, manifested in the long tails of the amplitude distribution. Moreover, we describe the two main mechanisms behind this effect. The first one, well-known in the literature, is due to random noise described by random matrix theory (RMT) and is commonly discarded as spurious, usually through some form of coarse graining procedure. The second one consists of algebraic lo-

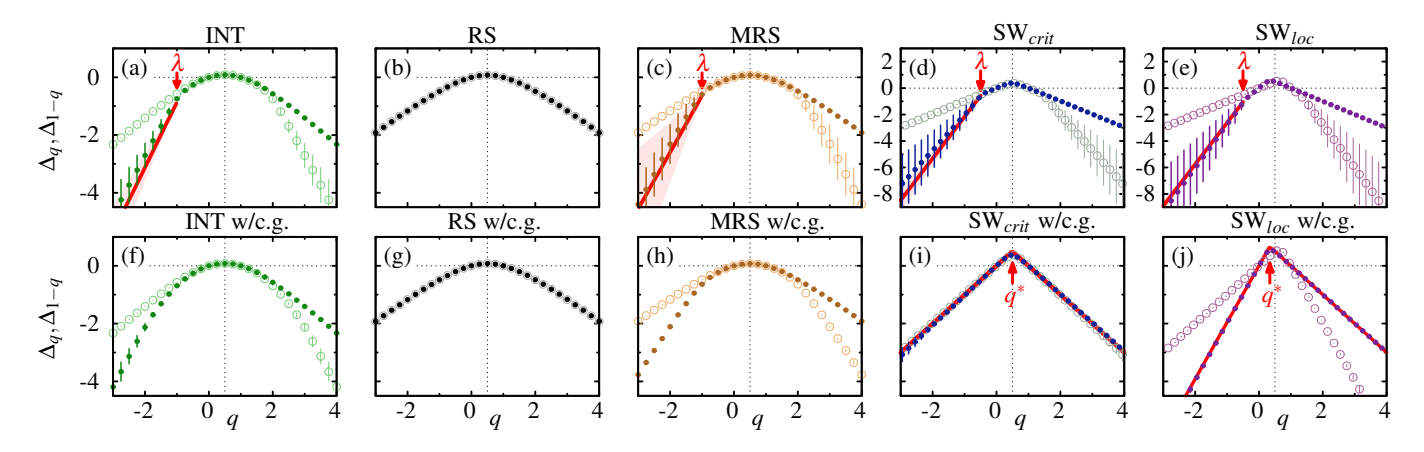


FIG. 1. Δ_q (solid circles) and Δ_{1-q} (empty circles) obtained from the scaling of the average moments $\sum_p \left\langle \left| \psi(p)^{2q} \right| \right\rangle \sim N^{1-q-\Delta_q}$ without coarse graining (top row) and with coarse graining (bottom row). The coarse graining parameter is $\ell=16$ for all but the SW model ($\ell=8$). The model parameters are $\gamma=1/3$ (INT), g=11/24 (RS), g=11/24, v=1 (MRS), W=16.75, p=0.49 (SW $_{\rm crit}$) and W=21, p=0.49 (SW $_{\rm loc}$). For the INT, RS and MRS models $N=2^{10},...,2^{14}$, and $2^{17}/N$ random realizations; for the SW model $N=2^{10},...,2^{20}$ and the number of realizations ranges from 4000 for the largest N to 27000 for the smallest (using 16 eigenvectors from each realization obtained using a highly optimized Jacobi-Davidson routine [37]). The red arrow (top row) marks the value of λ obtained from $P(\alpha) \sim N^{\lambda\alpha}$ for $\alpha \gtrsim 2$ [see Fig. 2]. The straight red (solid) lines (top row) shows the behavior for $q \lesssim \lambda$ predicted by Eq. (5) for large α . In (i) and (j), for the SW model, the arrows point to q^* which characterizes algebraic localization and the red (solid) lines show the predicted behavior $\Delta_q=q(1/q^*-1)$ for $q< q^*$ and $\Delta_q=1-q$ for $q>q^*$. In the critical case (i) $q^*=1/2$ and the symmetry holds.

calization. It is robust against coarse graining and appears as a characteristic signature of models strongly violating the multifractal symmetry.

The first model we consider is a 1D system periodically kicked by a discontinuous sawtooth potential whose Hamiltonian is $H = P^2 - \gamma\{X\}\sum_{n \in \mathbb{Z}} \delta(t-n)$, where $\{X\}$ is the fractional part of X, and γ is the kick amplitude. The stroboscopic dynamics at each period is given by the map $P_{n+1} = P_n + \gamma \pmod{1}$, $X_{n+1} = X_n + 2P_{n+1} \pmod{1}$. For irrational γ the system is ergodic [38] while for rational $\gamma \equiv a/b$ (with a,b coprime integers) the classical map is pseudointegrable [39]. In the latter case, the motion is periodic in momentum, with P taking only b different values.

The corresponding quantum map is [40, 41]

$$U_{pp'} = \frac{e^{i\phi_p}}{N} \frac{1 - e^{i2\pi\gamma/h}}{1 - e^{2i\pi(p' - p + \gamma/h)/N}},$$
 (3)

with $p = P/h \in \{0,...,N-1\}$, $\phi_p = -2\pi hp^2$, and h the effective Planck constant $h \equiv 1/N$. The semiclassical limit of this model is $N \to \infty$ ($h \to 0$). In order to get ensemble averages, we replace the phases ϕ_p by independent random variables uniformly distributed between 0 and 2π [42]. The level spacing statistics of this map is intermediate between Poisson and Wigner-Dyson: it has thus been dubbed the intermediate (INT) map. In correspondence with the classical dynamics, for γ irrational the eigenstates are extended [30, 36, 40], while for rational $\gamma = a/b$ and $N/b \notin \mathbb{Z}$ the eigenstates are multifractal [30, 35, 36, 43–45]. If we replace h by a finite number independent of N, (3) corresponds to the Ruijsenaars-Schneider (RS) ensemble of random matrices [46] parametrized by $g \equiv \gamma/h$. For the latter model, eigenstates are localized for g = 0, extended for $g \in \mathbb{Z}$, and

multifractal otherwise [30, 47, 48]. Varying $g \in (0,1)$ drives the system from strong to weak multifractality. The structure of the eigenstates of the INT map exhibits remnants of the classical dynamics (seen as b peaks in momentum) intertwined with multifractal fluctuations. In the RS ensemble, however, such a structure is not observed and multifractality is spatially homogeneous. Here we will show that the inhomogeneous multifractal properties present in the INT map are deeply connected with the violation of (2). The discrepancy in the behavior of these two closely related models will be analysed through a third model defined more precisely later below, the modulated RS (MRS) model, where eigenstates of the RS model are multiplied by an algebraically localized envelope.

Another system showing inhomogeneous multifractal properties corresponds to Anderson localization on random graphs [34, 49]. It has generated great interest recently due to its analogy to the many-body localization problem [17, 28, 33, 49–68]. Here, we consider an Anderson model on a small-world network (SW) [69], defined (for a fixed parameter *p*) by the Hamiltonian [70–72]

$$\hat{H} = \sum_{i=1}^{N} \left(\varepsilon_i |i\rangle \langle i| + |i\rangle \langle i+1| \right) + \sum_{k=1}^{\lfloor pN \rfloor} |i_k\rangle \langle j_k| + h.c., \quad (4)$$

corresponding to a chain of N sites (with periodic boundary conditions) with additional long-range links between $\lfloor pN \rfloor$ randomly chosen pairs of sites (i_k, j_k) with $|i_k - j_k| > 1$. The random on-site energies ε_i are sampled from a uniform distribution over [-W/2, W/2]. The graph topology of the model is locally treelike, with an average branching number $K \approx 1 + 2p$, and when $p \to 1/2$ it approaches a random regular graph. This model has recently been used to study Anderson localization on random graphs [34, 49]. For W larger than

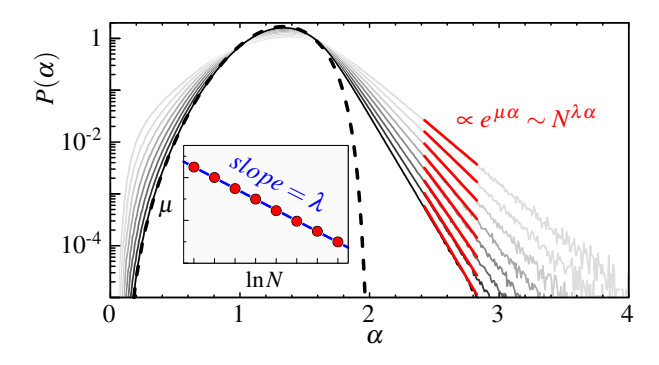


FIG. 2. Distribution $P(\alpha)$ for the rescaled eigenfunction amplitudes $\alpha = -\ln |\psi_p|^2 / \ln N$ for the RS (dashed lines) for g = 11/24 and $N = 2^{14}$, and the MRS (gray shaded lines) for g = 11/24, v = 1 and $N = 2^7, ..., 2^{14}$ (darker shade corresponds to larger N). The red solid lines show the exponential fit $P(\alpha) \propto e^{\mu \alpha}$ for large α characterizing the presence of atypically small values of $|\psi_p|^2$. Inset: Exponent μ vs. $\ln N$. A well-defined slope λ implies $P(\alpha) \sim N^{\lambda \alpha}$.

some $W_c(p)$ the system is localized, and presents a delocalization transition at $W = W_c(p)$. The localized phase has strong multifractality properties [73] and the symmetry (2) is known not to hold [29, 34].

Fig. 1 shows Δ_q (full circles) and Δ_{1-q} (empty circles) for these systems. Without coarse graining (top row) the symmetry is generally not valid for |q-1/2| large enough. This is true for other systems as well, such as the power-law random banded matrix (PRBM) model [19]. The only exception we observe is for the RS map, for which Eq. (2) holds perfectly well. The bottom row of Fig. 1 shows Δ_q when the wave functions are coarse grained over a small number of sites ℓ . In this case, Δ_q is extracted from the scaling of moments $\widetilde{I}_q = \sum_k \mu_k^q$, where $\mu_k = \sum_{r=0}^{\ell-1} |\psi_{k\ell+r}|^2$ gives the coarse-grained wave-function components. We observe that the coarse graining only restores the symmetry for the SW model at the critical point (SW_{crit}), whereas for the INT map and the SW in the localized regime (SW_{loc}) the violation of (2) persists.

For the INT and SW_{crit} models without coarse graining, the discontinuity in the derivative of Δ_q at q < 0 (indicated with a red arrow in Fig. 1) signals that the discrepancy comes from the small eigenfunction components. To verify this, we study the probability density function $P(\alpha)$ of $\alpha \equiv -\ln |\psi|^2 / \ln N$, a quantity that has been used for the study of critical wave function properties at the 3D Anderson transition [74-76]. In Fig. 2 we show $P(\alpha)$ for two of our models. For the RS model (which is the only one that is symmetric with and without coarse graining) $P(\alpha)$ (dashed line) vanishes for $\alpha > 2$. By contrast, for the MRS model (defined in detail below and representative of models with algebraic localization) $P(\alpha)$ shows exponential tails $P(\alpha) \sim N^{\lambda \alpha}$ for $\alpha \gtrsim 2$. We found such tails, with $\lambda < 0$ a system-dependent parameter, for all the other models [77]; they signify that atypically small wave function amplitudes exist for $\alpha \gtrsim 2$.

This feature is linked to the singular behavior of Δ_q at q < 0. Indeed, assuming $P(\alpha) \sim N^{\lambda \alpha + b}$ over a range $\bar{\alpha} < \alpha < \alpha_{\text{max}}$ one can show [77] that Δ_q for $q \lesssim \lambda$ is given by

$$\Delta_q = (q - \lambda)\alpha_{\text{max}} - q - b, \qquad q \lesssim \lambda.$$
(5)

In particular, this means that the Δ_q are affected asymmetrically (i.e. only for $q \lesssim \lambda$) by the exponential tail of $P(\alpha)$ at large α , and hence one can expect that (2) will in general not hold [78]. This is visible in Fig. 1, where red lines are (5) with the parameters extracted from the corresponding $P(\alpha)$.

We now turn to the two mechanisms leading to exponential tails in $P(\alpha)$ for the SW_{crit} and INT models: RMT Gaussian fluctuations pervading the smallest wave function components, and algebraic localization of eigenfunctions. The former is usually discarded through coarse graining [79]. However, the latter was not known, and is robust against coarse graining.

In the case where the smallest wave function components follow RMT [28], their distribution is given by the Porter-Thomas law [80], which implies $P(\alpha) \propto N^{\beta(1-\alpha)/2} \exp(-\frac{1}{2}\beta N^{1-\alpha})$, where $\beta = 1,2$ is the Dyson index corresponding to systems with or without timereversal symmetry, respectively [81]. For $\alpha > 1$ and $N \gg 1$, $\ln P(\alpha)$ is thus linear in α with a slope $-\frac{1}{2}\beta \ln N$, i.e. the type of behavior seen in Fig. 2 with λ given by $-\beta/2$. This is the situation for the SW_{crit} system, whose $P(\alpha)$ presents an exponential tail $P(\alpha) \sim N^{\lambda \alpha}$ with $\lambda = -1/2$. Time-reversal invariance of (4) indeed implies that Gaussian fluctuations are of GOE type, i.e. $\beta = 1$. As a consequence of Eq. (5), Δ_q displays a discontinuous change in steepness at $q \approx \lambda$, as can be seen in Fig. 1(d). The symmetry is recovered after coarse graining (Fig. 1(i)), in agreement with the fact that the Gaussian fluctuations are uncorrelated over sites. We note that in [29] a similar behavior is observed for $P(\alpha)$ at large α for the Cayley tree at the root (with $\beta = 2$ due to broken time-reversal invariance). Discarding that part of $P(\alpha)$, as is done in [29], leads to a symmetric Δ_q at the transition. Nevertheless, by taking into account the exponential tails at large α , a behavior like the one shown in Fig. 1(d) for Δ_a without coarse graining is found for the Cayley tree [77].

Let us now consider the second mechanism: algebraic localization. First, note that multifractality is a scale-invariant property. Therefore, it can be naturally expected that this specific type of localization can modify multifractal properties without destroying multifractality itself. Second, exponential tails $P(\alpha) \sim N^{\lambda \alpha}$ can arise from wave functions algebraically localized in the vicinity of some fixed point $P_0 \in (0,1)$. Indeed, consider a toy wave function ϕ with $|\phi(p)|^2 = A \left| \frac{p}{N} - P_0 \right|^V$ for $\left| \frac{p}{N} - P_0 \right| \ll 1$, with v > 0. One can straightforwardly relate the distribution F(u) of small $u(p) \equiv |\phi(p)|^2$ to the exponent v: if $p_{\pm}(u) = N \left[\pm (u/A)^{1/v} + P_0 \right] > 0$ is the inverse of u(p) around P_0 , then $F(u) \approx N^{-1}(p'_+(u) + p'_-(u)) \sim u^{1/v-1}$, and thus $P(\alpha) \sim N^{-\alpha/v}$ giving the exponential tails with $\lambda = -1/v$.

To better understand the interplay between the classical and the multifractal structure leading to the violation of Eq. (2) for the INT model, we construct the MRS model as follows. We combine RS eigenstates $\psi(p)$ with a smooth algebraically localized envelope $f_v(p/N)$ to obtain a vector $|\widetilde{\psi}(p)|^2 = A|\psi(p)|^2 f_v(p/N)$, where A is the normalization. We choose $f_v(p/N) = \left|\sin\left[\pi(\frac{p}{N}-P_0)\right]\right|^v$, with v=1 and $P_0 \in (0,1)$ drawn at random for each associated RS eigenstate. In Figs. 1(c) and 1(h) we show Δ_q for the MRS states. As expected from the above discussion, the symmetry is no longer verified. Moreover, $P(\alpha)$, displayed in Fig. 2 (solid grayscale lines), presents exponential tails $P(\alpha) \sim N^{-\alpha/v}$. As a consequence, Eq. (5) applies (see Fig. 1(c)). The modulation of the RS eigenstates with f_v thus leads to atypically small wave function components not previously present.

For the SW_{loc} system (i.e. (4) in the localized phase), the symmetry is also absent with and without coarse graining (Fig. 1 (e)-(j)). As observed from Fig. 1(j), it is due to the fact that the maximum of Δ_q has shifted away from q = 1/2, thereby precluding $\Delta_q = \Delta_{1-q}$. In this case, the origin of this behavior is an effective algebraic localization resulting from the interplay between the typical exponential localization of wave functions $e^{-r/\xi_{\rm typ}}$ around their localization center (with the localization length ξ_{typ} being the same in almost all directions) and the exponential proliferation K^r of sites at distance r [34]. Setting $R \equiv K^r$ and $q^* = \xi_{\text{typ}} \ln K$, we have $e^{-r/\xi_{\rm typ}}=R^{-1/q^*}$. The moments for such wave functions can then be rewritten as $I_q\sim \int_1^{N/K}dRR^{-q/q*}$, and thus they behave in the same way as for algebraically localized wave functions $|\psi_R|^2 \sim R^{-1/q^*}$ of a one-dimensional system of size $\sim N$, known to arise, e.g., for eigenstates of the supercritical PRBM model [82, 83]. The corresponding multifractal spectrum is $\Delta_q = q(1/q^* - 1)$ for $q < q^*$ and $\Delta_q = 1 - q$ for $q > q^*$, where $q^* < 1/2$ and $q^* \rightarrow 1/2$ as the transition is approached [29, 34]. This behavior is verified in Fig. 1(e)-(j). The position q^* of the maximum of Δ_q is related to the exponent $-1/q^*$ of the effective algebraic localization; it is also a singular point, in much the same way as to what happens for the algebraic envelope $f_{\nu}(x) \sim x^{\nu}$ of the MRS states, where the power $\nu > 0$ leads to non-analytic behavior of Δ_q at $q = -1/\nu < 0$.

The effective algebraic localization in the SW system is reflected in the typical correlation function $C_{\rm typ}(r) = \exp \langle \ln(\sum_i |\psi_i|^2 |\psi_{i+r}|^2) \rangle$ defined along the 1D lattice. As shown in [34], it decays as $C_{\rm typ}(r) \sim \exp(-r/\xi_{\rm typ}) = R^{-1/q^*}$, and therefore algebraically with the number $R = K^r$ of pairs of sites at a distance r of a given site.

The difference between Gaussian fluctuations and algebraic localization in the INT and RS models can also be visualized considering the average correlation function $C_q(r) = (N\langle |\psi|^{2q}\rangle)^{-1} \sum_{r'} \langle |\psi_{r'}|^q |\psi_{r'+r}|^q \rangle$. As we are interested in the smallest wave function components, in Fig. 3 we consider the case q < 0. Gaussian fluctuations are spatially uncorrelated and are therefore associated with a very low constant value of $C_{q<0}(r)$ for r>0. On the contrary, algebraic localization is associated with a power-law decay of the correlation function which enhances the usual algebraic decrease due to multifractality [27]. In Fig. 3, the MRS model (brown line) shows a faster algebraic decay than the RS model (black line),

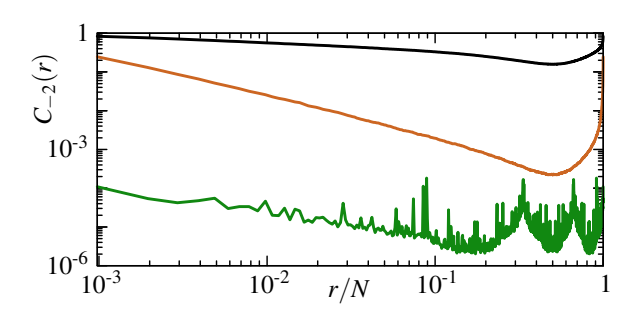


FIG. 3. Average correlation function $C_{-2}(r)$ in the RS (top, black), MRS (middle, brown), and INT models (bottom, green). System size is $N=2^{10}$ and number of random realizations 128. System parameters are g=11/24, v=1 and $\gamma=1/3$. Strong correlation in the RS model is associated with the cutoff in $P(\alpha)$ that favors the symmetry. Algebraic localization in MRS translates into less correlated eigenfunctions and violation of the symmetry. The INT map has both algebraic localization and Gaussian fluctuations.

an effect of the envelope f_v . The INT model (green line) has a similar decay as the MRS model, but multiplied by a very small constant prefactor, a signature of the presence of both algebraic localization and Gaussian fluctuations. In contrast, Gaussian fluctuations are absent in the RS model, consistent with the symmetry (2) holding without coarse graining.

In summary, we have studied the multifractal symmetry $\Delta_q = \Delta_{1-q}$ known to be valid for a large class of systems at criticality, and found two mechanisms that lead to its violation. The first one concerns atypically small wave function components that are due to Gaussian fluctuations at small scales. Though such fluctuations are known and eliminated by coarse graining, we showed that their precise characteristics can be obtained through their effect on multifractality. The second mechanism corresponds to algebraic localization of an otherwise homogeneously multifractal wave function that generates anomalously small values of $|\psi|^2$. In that case, the symmetry violation is robust to coarse graining.

We find that the robust violation of the multifractal symmetry is intrinsically related to *inhomogeneous* multifractal properties. For the Floquet critical system in the semiclassical regime our results suggest that the wave functions are modulated by an envelope with algebraic behavior around local minima, inducing a spatial inhomogeneity of the multifractal fluctuations without destroying their characteristic scale invariance. We interpret this envelope as similar to EBK envelopes [84], localized around regular tori in integrable systems.

Anderson localization in random graphs is also associated with an effective algebraic localization due to the interplay between the exponential localization of wave functions and the exponential growth of available sites, leading to strong multifractality in the localized phase where the symmetry relation is not respected. The non-ergodic properties of this problem have been much discussed recently in relation to the many-body localization problem [28, 33, 49–58, 60–67], the Cayley tree [29, 33, 58, 59, 61] and certain types of random matrices

[56, 64, 85–87]. Also, the MBL phase [12, 13] and many-body eigenstates [8–11] are generically multifractal in Hilbert space. It would be interesting to study these important problems along the lines of this Letter.

This study has been (partially) supported through the EUR grant NanoX ANR-17-EURE-0009 in the framework of the "Programme des Investissements d'Avenir", the French-Argentinian LIA LICOQ, and also by research funding Grants No. ANR-17-CE30-0024, ANR-18-CE30-0017 and ANR-19-CE30-0013. We thank Calcul en Midi-Pyrénées (CALMIP) for computational resources and assistance. A.M.B. is grateful to Nicolas Macé for valuable technical advice concerning the numerical computations, and to Pablo Kaluza for useful discussions. I.G.-M. received funding from CONICET (Grant No. PIP 11220150100493CO) and ANCyPT (Grant No. PICT-2016-1056).

- P. W. Anderson, Absence of diffusion in certain random lattices, Phys. Rev. 109, 1492 (1958).
- [2] F. Evers and A. D. Mirlin, Anderson transitions, Rev. Mod. Phys. 80, 1355 (2008).
- [3] B. B. Mandelbrot, Intermittent turbulence in self-similar cascades: divergence of high moments and dimension of the carrier, J. Fluid Mech. **62**, 331 (1974).
- [4] B. B. Mandelbrot, *The fractal geometry of nature*, Vol. 2 (WH freeman New York, 1982).
- [5] K. Falconer, Fractal geometry: mathematical foundations and applications (John Wiley & Sons, Chichester, 1990).
- [6] Y. Y. Atas and E. Bogomolny, Multifractality of eigenfunctions in spin chains, Phys. Rev. E **86**, 021104 (2012).
- [7] Y. Atas and E. Bogomolny, Calculation of multi-fractal dimensions in spin chains, Philosophical Transactions of the Royal Society A: Mathematical, Physical and Engineering Sciences 372, 20120520 (2014).
- [8] D. J. Luitz, F. Alet, and N. Laflorencie, Universal behavior beyond multifractality in quantum many-body systems, Phys. Rev. Lett. 112, 057203 (2014).
- [9] J. Lindinger and A. Rodríguez, Multifractality in fock space of the ground state of the bose-hubbard hamiltonian, Acta Physica Polonica A 132, 1683 (2017).
- [10] J. Lindinger, A. Buchleitner, and A. Rodríguez, Many-body multifractality throughout bosonic superfluid and mott insulator phases, Phys. Rev. Lett. 122, 106603 (2019).
- [11] L. Pausch, E. G. Carnio, A. Rodríguez, and A. Buchleitner, Chaos and ergodicity across the energy spectrum of interacting bosons, arXiv preprint arXiv:2009.05295 (2020).
- [12] N. Macé, F. Alet, and N. Laflorencie, Multifractal scalings across the many-body localization transition, Phys. Rev. Lett. 123, 180601 (2019).
- [13] M. Tarzia, Many-body localization transition in hilbert space, Phys. Rev. B 102, 014208 (2020).
- [14] D. A. Abanin, E. Altman, I. Bloch, and M. Serbyn, Colloquium: Many-body localization, thermalization, and entanglement, Reviews of Modern Physics 91, 021001 (2019).
- [15] F. Alet and N. Laflorencie, Many-body localization: An introduction and selected topics, Comptes Rendus Physique 19, 498 (2018).
- [16] D. A. Abanin and Z. Papić, Recent progress in many-body lo-

- calization, Annalen der Physik 529, 1700169 (2017).
- [17] K. Tikhonov and A. Mirlin, From Anderson localization on random regular graphs to many-body localization, arXiv preprint arXiv:2102.05930 (2021).
- [18] V. N. Smelyanskiy, K. Kechedzhi, S. Boixo, S. V. Isakov, H. Neven, and B. Altshuler, Nonergodic delocalized states for efficient population transfer within a narrow band of the energy landscape, Phys. Rev. X 10, 011017 (2020).
- [19] A. Mirlin, Y. V. Fyodorov, A. Mildenberger, and F. Evers, Exact relations between multifractal exponents at the Anderson transition, Phys. Rev. Lett. 97, 046803 (2006).
- [20] I. Gruzberg, A. Ludwig, A. Mirlin, and M. Zirnbauer, Symmetries of multifractal spectra and field theories of Anderson localization, Phys. Rev. Lett. 107, 086403 (2011).
- [21] I. A. Gruzberg, A. Mirlin, and M. Zirnbauer, Classification and symmetry properties of scaling dimensions at Anderson transitions, Phys. Rev. B 87, 125144 (2013).
- [22] C. Monthus, B. Berche, and C. Chatelain, Symmetry relations for multifractal spectra at random critical points, Journal of Statistical Mechanics: Theory and Experiment 2009, P12002 (2009).
- [23] A. Mildenberger and F. Evers, Wave function statistics at the symplectic two-dimensional Anderson transition: Bulk properties, Phys. Rev. B 75, 041303 (2007).
- [24] H. Obuse, A. R. Subramaniam, A. Furusaki, I. A. Gruzberg, and A. W. Ludwig, Multifractality and conformal invariance at 2D metal-insulator transition in the spin-orbit symmetry class, Phys. Rev. Lett. 98, 1 (2007), 0609161.
- [25] L. J. Vasquez, A. Rodriguez, and R. A. Römer, Multifractal analysis of the metal-insulator transition in the three-dimensional Anderson model. I. Symmetry relation under typical averaging, Phys. Rev. B 78, 195106 (2008).
- [26] A. Rodriguez, L. J. Vasquez, and R. A. Römer, Multifractal analysis of the metal-insulator transition in the three-dimensional Anderson model. II. Symmetry relation under ensemble averaging, Phys. Rev. B Condensed Matter and Materials Physics 78, 1 (2008), 0807.2217.
- [27] F. Evers, A. Mildenberger, and A. D. Mirlin, Multifractality at the quantum hall transition: Beyond the parabolic paradigm, Phys. Rev. Lett. 101, 10.1103/PhysRevLett.101.116803 (2008).
- [28] A. De Luca, B. Altshuler, V. Kravtsov, and A. Scardicchio, Anderson localization on the Bethe lattice: nonergodicity of extended states, Phys. Rev. Lett. 113, 046806 (2014).
- [29] K. S. Tikhonov and A. D. Mirlin, Fractality of wave functions on a Cayley tree: Difference between tree and locally treelike graph without boundary, Phys. Rev. B 94, 184203 (2016).
- [30] E. Bogomolny and O. Giraud, Multifractal dimensions for all moments for certain critical random-matrix ensembles in the strong multifractality regime, Phys. Rev. E 85, 046208 (2012).
- [31] V. Kravtsov, I. Khaymovich, E. Cuevas, and M. Amini, A random matrix model with localization and ergodic transitions, New Journal of Physics 17, 122002 (2015).
- [32] S. Faez, A. Strybulevych, J. H. Page, A. Lagendijk, and B. A. Van Tiggelen, Observation of multifractality in Anderson localization of ultrasound, Phys. Rev. Lett. 103, 7 (2009), 0906.1173.
- [33] M. Sonner, K. S. Tikhonov, and A. D. Mirlin, Multifractality of wave functions on a Cayley tree: From root to leaves, Phys. Rev. B 96, 1 (2017), 1708.04978.
- [34] I. García-Mata, J. Martin, R. Dubertrand, O. Giraud, B. Georgeot, and G. Lemarié, Two critical localization lengths in the Anderson transition on random graphs, Phys. Rev. Research 2, 012020 (2020).
- [35] J. Martin, O. Giraud, and B. Georgeot, Multifractality and inter-

- mediate statistics in quantum maps, Phys. Rev. E 77, 035201(R) (2008)
- [36] J. Martin, I. García-Mata, O. Giraud, and B. Georgeot, Multi-fractal wave functions of simple quantum maps, Phys. Rev. E 82, 046206 (2010).
- [37] M. Bollhöfer and Y. Notay, Jadamilu: a software code for computing selected eigenvalues of large sparse symmetric matrices, Computer Physics Communications 177, 951 (2007).
- [38] H. Furstenberg, Strict ergodicity and transformation of the torus, American Journal of Mathematics 83, 573 (1961).
- [39] P. Richens and M. Berry, Pseudointegrable systems in classical and quantum mechanics, Physica D: Nonlinear Phenomena 2, 495 (1981).
- [40] J. Marklof and Z. Rudnick, Quantum unique ergodicity for parabolic maps, Geometric & Functional Analysis GAFA 10, 1554 (2000).
- [41] O. Giraud, J. Marklof, and S. O'Keefe, Intermediate statistics in quantum maps, J. Phys. A: Math. Gen. 37, L303 (2004).
- [42] E. Bogomolny and C. Schmit, Spectral statistics of a quantum interval-exchange map, Phys. Rev. Lett. 93, 254102 (2004).
- [43] R. Dubertrand, I. García-Mata, B. Georgeot, O. Giraud, G. Lemarié, and J. Martin, Two scenarios for quantum multifractality breakdown, Phys. Rev. Lett. 112, 234101 (2014).
- [44] R. Dubertrand, I. García-Mata, B. Georgeot, O. Giraud, G. Lemarié, and J. Martin, Multifractality of quantum wave functions in the presence of perturbations, Phys. Rev. E 92, 032914 (2015).
- [45] A. M. Bilen, I. García-Mata, B. Georgeot, and O. Giraud, Multifractality of open quantum systems, Phys. Rev. E 100, 032223 (2019).
- [46] E. Bogomolny, O. Giraud, and C. Schmit, Random matrix ensembles associated with lax matrices, Phys. Rev. Lett. 103, 054103 (2009).
- [47] I. García-Mata, J. Martin, O. Giraud, and B. Georgeot, Multi-fractality of quantum wave packets, Phys. Rev. E 86, 056215 (2012).
- [48] E. Bogomolny and O. Giraud, Eigenfunction entropy and spectral compressibility for critical random matrix ensembles, Phys. Rev. Lett. 106, 044101 (2011).
- [49] I. García-Mata, O. Giraud, B. Georgeot, J. Martin, R. Dubertrand, and G. Lemarié, Scaling theory of the Anderson transition in random graphs: ergodicity and universality, Phys. Rev. Lett. 118, 166801 (2017).
- [50] R. Abou-Chacra, D. Thouless, and P. Anderson, A selfconsistent theory of localization, Journal of Physics C: Solid State Physics 6, 1734 (1973).
- [51] C. Castellani, C. Di Castro, and L. Peliti, On the upper critical dimension in Anderson localisation, J. Phys. A: Math. Gen. 19, L1099 (1986).
- [52] A. D. Mirlin and Y. V. Fyodorov, Distribution of local densities of states, order parameter function, and critical behavior near the Anderson transition, Phys. Rev. Lett. 72, 526 (1994).
- [53] C. Monthus and T. Garel, Anderson transition on the Cayley tree as a traveling wave critical point for various probability distributions, J. Phys. A: Math. Theo. 42, 075002 (2008).
- [54] G. Biroli, A. Ribeiro-Teixeira, and M. Tarzia, Difference between level statistics, ergodicity and localization transitions on the Bethe lattice, arXiv preprint arXiv:1211.7334 (2012).
- [55] C. Monthus and T. Garel, Anderson localization on the Cayley tree: multifractal statistics of the transmission at criticality and off criticality, J. Phys. A: Math. Theo. 44, 145001 (2011).
- [56] D. Facoetti, P. Vivo, and G. Biroli, From non-ergodic eigenvectors to local resolvent statistics and back: A random matrix perspective, EPL (Europhysics Lett.) 115, 47003 (2016).

- [57] G. Parisi, S. Pascazio, F. Pietracaprina, V. Ros, and A. Scardicchio, Anderson transition on the Bethe lattice: an approach with real energies, J. Phys. A: Math. Theo. 53, 014003 (2019).
- [58] V. E. Kravtsov, B. L. Altshuler, and L. B. Ioffe, Non-ergodic delocalized phase in Anderson model on Bethe lattice and regular graph, Ann. Phys. 389, 148 (2018).
- [59] S. Savitz, C. Peng, and G. Refael, Anderson localization on the Bethe lattice using cages and the wegner flow, Phys. Rev. B 100, 094201 (2019).
- [60] K. Tikhonov, A. Mirlin, and M. Skvortsov, Anderson localization and ergodicity on random regular graphs, Phys. Rev. B 94, 220203 (2016).
- [61] G. Biroli and M. Tarzia, Delocalization and ergodicity of the Anderson model on Bethe lattices, arXiv preprint arXiv:1810.07545 (2018).
- [62] K. Tikhonov and A. Mirlin, Statistics of eigenstates near the localization transition on random regular graphs, Phys. Rev. B 99, 024202 (2019).
- [63] K. Tikhonov and A. Mirlin, Critical behavior at the localization transition on random regular graphs, Phys. Rev. B 99, 214202 (2019).
- [64] V. E. Kravtsov, I. M. Khaymovich, E. Cuevas, and M. Amini, A random matrix model with localization and ergodic transitions, New Journal of Physics 17, 10.1088/1367-2630/17/12/122002 (2015), 1508.01714.
- [65] B. Altshuler, E. Cuevas, L. Ioffe, and V. Kravtsov, Nonergodic phases in strongly disordered random regular graphs, Phys. Rev. Lett. 117, 156601 (2016).
- [66] S. Bera, G. De Tomasi, I. M. Khaymovich, and A. Scardicchio, Return probability for the Anderson model on the random regular graph, Phys. Rev. B 98, 134205 (2018).
- [67] G. Biroli and M. Tarzia, Delocalized glassy dynamics and many-body localization, Phys. Rev. B 96, 201114 (2017).
- [68] F. L. Metz, G. Parisi, and L. Leuzzi, Finite-size corrections to the spectrum of regular random graphs: An analytical solution, Phys. Rev. E 90, 052109 (2014).
- [69] D. J. Watts and S. H. Strogatz, Collective dynamics of 'small-world' networks, Nature 393, 440 (1998).
- [70] C.-P. Zhu and S.-J. Xiong, Localization-delocalization transition of electron states in a disordered quantum small-world network, Phys. Rev. B 62, 14780 (2000).
- [71] C.-P. Zhu and S.-J. Xiong, Fractal analysis of wave functions at the localization-delocalization transition in a disordered quantum small-world-network model, Phys. Rev. B 63, 193405 (2001).
- [72] O. Giraud, B. Georgeot, and D. L. Shepelyansky, Quantum computing of delocalization in small-world networks, Phys. Rev. E 72, 036203 (2005).
- [73] The localization properties here are distinct from what happens in finite dimensionality where localization implies, in particular, an *exponential* decay of the wave function.
- [74] A. Rodriguez, L. J. Vasquez, and R. A. Römer, Multifractal analysis with the probability density function at the three-dimensional Anderson transition, Phys. Rev. Lett. 102, 106406 (2009).
- [75] A. Rodriguez, L. J. Vasquez, K. Slevin, and R. A. Römer, Critical parameters from a generalized multifractal analysis at the Anderson transition, Phys. Rev. Lett. 105, 1 (2010).
- [76] A. Rodriguez, L. J. Vasquez, K. Slevin, and R. A. Römer, Multi-fractal finite-size scaling and universality at the Anderson transition, Phys. Rev. B 84, 134209 (2011).
- [77] A. M. Bilen, B. Georgeot, O. Giraud, G. Lemarié, and I. García-Mata, in preparation (2021).
- [78] A. M. Bilen, B. Georgeot, O. Giraud, G. Lemarié, and I. García-

- Mata, Supplemental Material (2021).
- [79] See [28] for an alternative procedure to get rid of these fluctuations
- [80] C. E. Porter and R. G. Thomas, Fluctuations of nuclear reaction widths, Phys. Rev. 104, 483 (1956).
- [81] M. L. Mehta, Random matrices (Elsevier, 2004).
- [82] C. Yeung and Y. Oono, A conjecture on nonlocal random tightbinding models, EPL (Europhysics Lett.) 4, 1061 (1987).
- [83] A. D. Mirlin, Y. V. Fyodorov, F.-M. Dittes, J. Quezada, and T. H. Seligman, Transition from localized to extended eigenstates in the ensemble of power-law random banded matrices, Phys. Rev. E 54, 3221 (1996).
- [84] M. V. Berry, Semi-classical mechanics in phase space: a study of wigner's function, Phil. Trans. R. Soc. A. 287, 237 (1977).
- [85] I. M. Khaymovich, V. E. Kravtsov, B. L. Altshuler, and L. B. Ioffe, Fragile extended phases in the log-normal Rosenzweig-Porter model, Phys. Rev. Research 2, 043346 (2020).
- [86] G. Biroli and M. Tarzia, The Lévy-Rosenzweig-Porter random matrix ensemble, arXiv preprint arXiv:2012.12841 (2020).
- [87] E. Bogomolny and O. Giraud, Statistical properties of structured random matrices, arXiv preprint arXiv:2012.14322 (2020).

SUPPLEMENTAL MATERIAL

$P(\alpha)$ at large α and symmetry of Δ_a

In this section we discuss in more detail the relationship between the distribution $P(\alpha)$ and the symmetry $\Delta_q = \Delta_{1-q}$.

We first observe that the distribution $P(\alpha)$ at large α affects Δ_q at small q. In particular, when $P(\alpha) \sim N^{\lambda \alpha + b}$ for $\alpha \in [\bar{\alpha}, \alpha_{max}]$, with $\lambda < 0$, we have $\Delta_q = (q - \lambda)\alpha_{max} - q - b$ for $q \lesssim \lambda < 0$ (see Eq. (5)). Thus, the function Δ_q in this region $q \lesssim \lambda < 0$ can be expressed in terms of the parameters λ and b that govern the algebraic tail of $P(\alpha)$ at $\alpha > \bar{\alpha}$. For q > 0, on the other hand, the behavior of Δ_q is dependent only on the properties of $P(\alpha)$ for $\alpha < \bar{\alpha}$. As a consequence, given a Δ_q that satisfies the symmetry $\Delta_q = \Delta_{1-q}$, any modification of $P(\alpha)$ on one side of $\bar{\alpha}$ only will result in the violation of this symmetry.

Suppose now that we have two systems for which the distributions $P(\alpha)$ coincide for $\alpha < \bar{\alpha}$, but with $P(\alpha)$ vanishing at $\alpha > \bar{\alpha}$ for one of them and $P(\alpha) \sim N^{\lambda \alpha}$ at $\alpha > \bar{\alpha}$ for the other one. This is illustrated in Fig. 2 of the main text, where the dashed line vanishes at $\bar{\alpha} = 2$ while the solid lines display power-law tails beyond that value. It follows from the considerations above that if one of these systems satisfies the symmetry $\Delta_q = \Delta_{1-q}$ then the other one will not.

An instance of this is precisely given by the models whose distributions are displayed in Fig. 2: the Ruijsenaars-Schneider (RS) random matrix model and the modulated Ruijsenaars-Schneider (MRS) vector ensemble. As can be seen in Fig. 2 the $P(\alpha)$ at $\alpha \lesssim 2$ are almost identical (and all the more so as N gets larger), whereas for $\alpha \gtrsim 2$ the distribution vanishes for the RS model while it behaves as $P(\alpha) \sim N^{\lambda \alpha}$ for the MRS model. Since Δ_q is symmetric for the RS model, this implies the violation of the symmetry for the MRS model. This is confirmed by the plots in Fig. 1(b) and Fig. 1(c).

Another example is the small-world model at criticality (SW_{crit}), where coarse graining only affects the tail of $P(\alpha)$ at $\alpha > \bar{\alpha}$. Since with coarse graining the symmetry holds, in the absence of it the symmetry breaks down (see Fig. 1(d) and 1(i)). In the RS model, the coarse graining does not affect $P(\alpha)$ for $\alpha > \bar{\alpha}$ and the symmetry remains valid.